



ELSEVIER

Infrared Physics & Technology xxx (2002) xxx–xxx

 INFRARED PHYSICS
& TECHNOLOGY

www.elsevier.com/locate/infrared

Heat losses and 3D diffusion phenomena for defect sizing procedures in video pulse thermography

N. Ludwig *, P. Teruzzi

Dipartimento di Fisica, Institute of General Applied Physics, via Celoria 16, 20133 Milano, Italy

Abstract

Dynamical thermographic techniques like video pulse thermography are very useful for the non-destructive testing of structural components. In literature different models were proposed, which allow to describe the time evolution of the thermal contrast for materials with sub-superficial defects. In the case of circular defect the time evolution of the full width half maximum (FWHM) of the thermal contrast was studied both theoretically and experimentally. Nevertheless a mismatch in defect sizing between experimental results and theoretical simulations was found. Possible explanations of this disagreement was analysed. A factor widely neglected is the heat loss (radiation and convection). In this paper a theoretical analysis of the influence of these contributions is reported. Furthermore in order to explain the experimental evidence of FWHM time evolution we introduced a correction due to lateral heat diffusion around the defect. In this way a possible explanation for the experimental results was obtained. Brick samples with a circular flat bottom hole as defect was tested both for the interest in defect sizing in building material through NDT and for the low thermal diffusivity of this material which allows the study of the phenomenon in a slow motion. © 2002 Published by Elsevier Science B.V.

Keywords: Video pulse thermography; Defect sizing; Low diffusivity materials

1. Introduction

Nowadays the main topic of research in transient thermography is related to the development of suitable analytical models representing on the sample surface the spatial distribution of the thermal contrast (the difference of temperature between a defect region and a sound one) vs. time after the heating pulse. The availability of analytical solutions of the heat conduction law in solids in the presence of sub-surface defects would allow

the resolution of the inverse problem, which is to obtain information on the defect geometry, typically area and depth, from the sequence of infrared images of the sample surface recorded during the cooling. Starting from theoretical models of heat diffusion, algorithms have been proposed to estimate defect size. In particular, the one proposed by Crowther et al. [1] is easy to use even if it is useful only for circular defects. In this simple case the time evolution of the full width half maximum (FWHM) of the thermal contrast on the defect was studied both theoretically and experimentally. An algorithm proposed [2], in order to evaluate the diameter of a sub-surface circular cracklike defect, appears very attractive because it requires only the

* Corresponding author. Tel.: +39-2-5835-7473; fax: +39-2-5835-7422.

E-mail address: nicola.ludwig@unimi.it (N. Ludwig).

2

N. Ludwig, P. Teruzzi / Infrared Physics & Technology xxx (2002) xxx-xxx

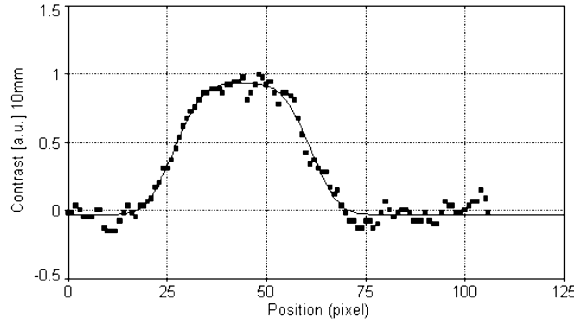


Fig. 1. Spatial profile of thermal contrast along diameter.

45 measurement at different times of the FWHM of
 46 the shape temperature difference distribution on
 47 the sample surface above the defect (Fig. 1). The
 48 extrapolation at the initial time (at the pulse
 49 starting) of the FWHM gives the true value of the
 50 defect diameter [3].

51 The aforesaid model allows to estimate the time
 52 evolution of FWHM of thermal contrast. In the
 53 model considered [1] every point of the medium is
 54 represented as a thermal wave front source whose
 55 evolution is described by a point-spread-function
 56 (PSF). This is a convolution integral between the
 57 Green function for the Fourier's problem for a
 58 semi-infinite medium and the temperature dis-
 59 tribution in such a medium. We stress that the
 60 expression for the distribution above is given by

$$T_0(r, t) = \frac{Q}{\varepsilon} \frac{1}{\sqrt{\pi t}} \exp\left(-\frac{z^2}{4xt}\right) \quad (1)$$

62 where spatial dependence is given only by the co-
 63 ordinate z normal to defect plane. In our case the
 64 studied model represents the defect as a group of
 65 equivalent heat source points in order to describe

the time dependence of the spatial distribution of
 the thermal contrast on the surface. The value of
 the thermal contrast in a general point r of the
 surface at time t is

$$C(r, t) \cong -\frac{Q}{2\pi(\pi x t)^{1/2}} \frac{\partial}{\partial L} \int_{-\infty}^{+\infty} \int_{-\infty}^{+\infty} dx' dy' \exp\left(-\left\{\left[(x-x')^2 + (y-y')^2 + L^2\right]^{1/2} + L\right\}^2 / 4xt\right) \times \frac{f(x', y')}{\left[(x-x')^2 + (y-y')^2 + L^2\right]^{1/2}} \quad (2)$$

where the convolution operates on the PSF on the
 top-hat $f(x, y)$ function

$$f(x', y') = \begin{cases} 1 & (x', y') \in D \\ 0 & (x', y') \notin D \end{cases} \quad (3)$$

which describes the defect region D . In the defect
 centre the solution for this integral (2) was still
 proposed in '98 [4]. It shows a good agreement
 with experimental results. On the other hand no
 models give an exact representation of the time
 evolution of the defect thermal shape evaluated
 along a line lying on diameter of the defect. This
 represents a true limit to the defect sizing using
 analytical models. A mismatch between experi-
 mental results and theoretical simulations was
 found. In fact, the experimental values of FWHM
 of the thermal contrast show a linear decrease vs.
 square root time while the model outlines a growth
 of these values after the time of maximum contrast
 (Fig. 2) [5]. In order to explicate this experimen-
 tal behaviour an empirical algorithm was proposed by
 Almond and Lau [3]. In this way the authors in-
 troduced some modifications to the studied model,
 in particular an experimental set up apt to evaluate

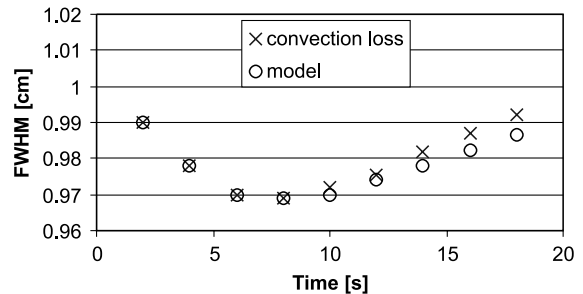
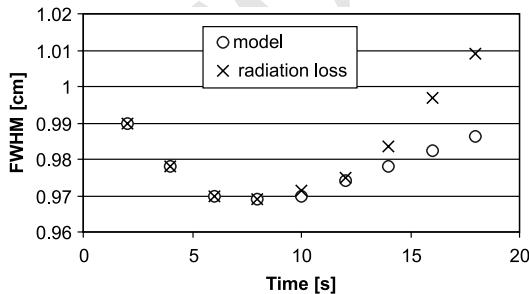


Fig. 2. FWHM time evolution of the thermal contrast above a defect for the adiabatic model (O) and with dissipation terms (X).

93 the extreme forced convection effect was studied
 94 [6]. No particularly remarkable results were ob-
 95 tained. In this study we operated with low diffu-
 96 sivity materials (stone, brick) which are interesting
 97 within the field of NDT on historic architecture.
 98 Furthermore we stress that in this way we also
 99 optimise the features of thermographical proced-
 100 ures by exploiting the slow time characteristic of
 101 heat diffusion ($3.5 \times 10^{-7} \text{ m}^2/\text{s}$) in these materials.

102 **2. Heat losses in video pulse thermography**

103 At first we considered the importance of dissi-
 104 pative terms (convection and radiation) which
 105 were neglected in previous studies. These losses
 106 were introduced in the aforesaid model and their
 107 influence on the superficial thermal distribution
 108 was evaluated by computing simulation. In par-
 109 ticular the heat losses were introduced by modi-
 110 fying the matrix of energy density in the
 111 computing analysis in order to calculate the inte-
 112 gral of thermal contrast.

113 *Radiation term:* the radiation contribution to
 114 heat losses in a step of Δt length was considered
 115 taking into account the expression of the radiant
 116 energy

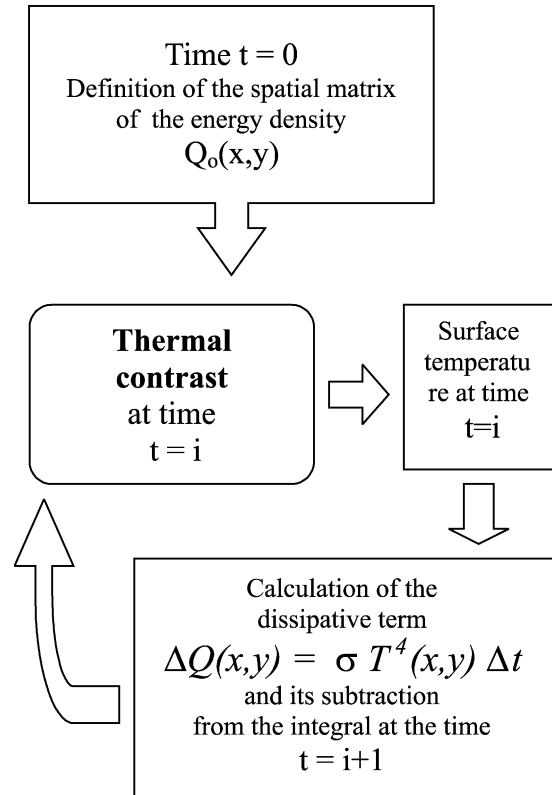
$$\Delta Q(x, y) = F \varepsilon \sigma T^4(x, y) \Delta t \quad (4)$$

118 where F is the radiant shape factor for a plane
 119 surface and ε its emissivity. This term calculates
 120 for every time the temperature distribution of the
 121 medium surface by a subtraction from the energy
 122 distribution in the previous step as shown in
 123 Scheme 1.

124 *Convection* is a further term which dissipates
 125 energy. It takes into account the difference be-
 126 tween the superficial temperature above the defect
 127 region and the sound one. We introduced this term
 128 depending on the air/sample temperature differ-
 129 ence and the convection coefficient h as [7]:

$$\Delta Q(x, y) = h(T_{\text{sup}} - T_{\text{air}})(x, y) \Delta t \quad (5)$$

131 This term redefines at every step the temperature
 132 distribution of the sample surface by an oportune
 133 subtraction from the energy distribution used in
 134 the previous step in a way similar to Scheme 1. In



Scheme 1.

both cases no remarkable variation in the behav- 135
 iour of thermal contrast was obtained. 136

137 **3. Lateral heat transfer**

138 At this point we stressed that the model reduced 138
 the heat transfer to a one-dimensional (1D) 139
 problem based on the aforesaid solution (1) for a 140
 semi-infinite medium [1]. As a consequence the 141
 effects of the PSF are the same for every point in 142
 the medium, except for the defect zone whose 143
 points differ from the others only for a multipli- 144
 cative factor. However this assumption does not 145
 assure the lateral heat transfer from the warmer 146
 zone above the defect to the boundary zones. In 147
 order to evaluate this effect we propose an ana- 148
 lytical modification to the top-hat shape in the 149
 formula (2). In the updated 2D-cylindrical model 150
 schematically we represented the warmer zone in 151

4

N. Ludwig, P. Teruzzi / Infrared Physics & Technology xxx (2002) xxx-xxx

152 the sample, above the defect, as a cylinder of ra-
 153 dius R_i that spreads heat into a larger cylinder of
 154 radius R_e . At any further time, R_i and R_e are re-
 155 defined depending on the propagation of the heat
 156 front in the medium, as shown in the following
 157 formulas:

$$\begin{aligned} R_i(t_{k+1}) &= R_i(t_k) - k_D \mu \text{ and } R_e(t_{k+1}) \\ &= R_e(t_k) + k_D \mu \end{aligned} \quad (6)$$

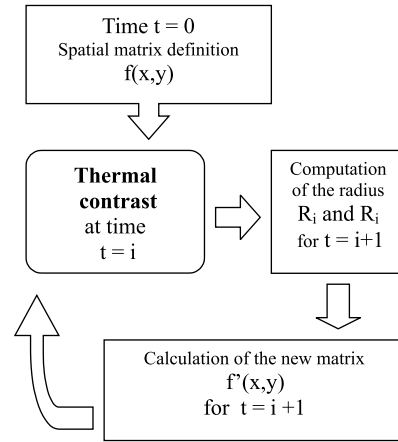
159 Where μ is the thermal diffusion length in video
 160 pulse thermography (PVT) [3] and k_D a propor-
 161 tionality coefficient < 1 . In this approach μ is a
 162 reference to the maximum possible length of the
 163 radius variation inside the medium in a temporal
 164 step. The new shape of the source point distribu-
 165 tion between R_i and R_e is defined step by step by
 166 the solution of the Fourier's problem for steady-
 167 state conduction in cylinder symmetry. This ap-
 168 proximation for the steady-state condition was
 169 assumed because of the very little temporal step
 170 considered in the computing.

$$f(i, j) = \begin{cases} 1 & \text{for } r(i, j) \leq R_i \\ 1 - \frac{\ln(r(i, j)/R_i)}{\ln(R_e/R_i)} & \text{for } R_i < r(i, j) < R_e \\ 0 & \text{for } r(i, j) \geq R_e \end{cases} \quad (7)$$

172 This correction of the PSF formula was introduced
 173 in the simulation summarised schematically in
 174 Scheme 2.

175 4. Results

176 The correction proposed here allows to obtain a
 177 modification in the FWHM behaviour as expected



Scheme 2.

from the comparison with the experimental data 178
 (Fig. 3a). The temporal evolution evaluated at the 179
 defect centre is still satisfied. Furthermore the 180
 FWHM evolution obtained from the calculations 181
 shown in Fig. 3b verifies the linear decrease of 182
 experimental data in Fig. 3a. 183

184 5. Conclusions

185 Although this work refers to a very limited field 185
 (low diffusivity materials, circular defects) and the 186
 approach is quite empirical, the authors wish show 187
 a way to identify physical phenomena which have 188
 importance in determining temperature evolution 189
 on the surface in the sub-superficial defect detec- 190
 tion with PVT techniques. We demonstrated how 191
 the lateral heat transfer influences the FWHM of 192

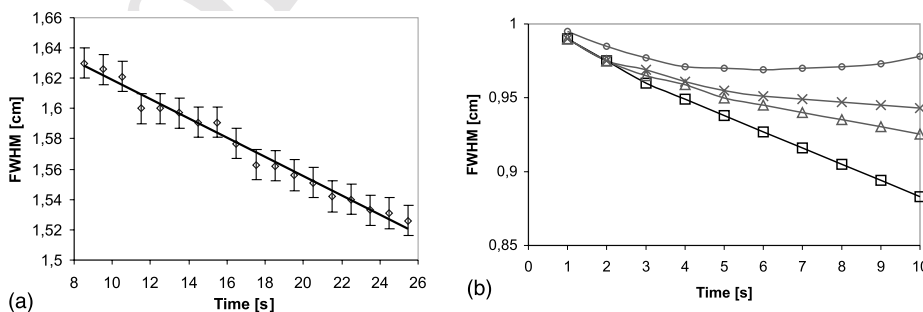


Fig. 3. (a) Experimental values of FWHM vs. time, and (b) comparison between FWHM time evolution obtained from formula (2) (○) and its correction obtained considering lateral heat losses with increasing values of k_D : 1/5 (×), 1/4 (△) and 1/3 (□).

193 the thermal contrast. This model can be usefully
 194 improved with the introduction of more precise
 195 corrections and further experimental verifications
 196 even with materials with different thermal charac-
 197 teristics.

198 References

- 199 [1] D.J. Crowther, L.D. Favro, P.K. Kuo, R.L. Thomas,
 200 Inverse scattering algorithm applied to infrared thermal
 201 wave images, *J. Appl. Phys.* 74 (9) (1993).
 202 [2] M.B. Saintey, D.P. Almond, Defect sizing by transient
 203 thermography. II: an numerical treatment, *J. Phys. D: Appl.*
 204 *Phys.* 28 (1995).
 205 [3] D.P. Almond, S.K. Lau, Defect sizing by transient ther-
 206 mography. I: an analytical treatment, *J. Phys. D: Appl.*
 207 *Phys.* 27 (1994).

- [4] F. Cernuschi, S. Ghia, N. Ludwig, A. Russo, P. Teruzzi, 208
 Una nuova metodologia per il dimensionamento dei difetti
 209 subsuperficiali con la termografia impulsata 9th Nat. Congr.
 210 AIPND. Padova, 1997. 211
 [5] F. Cernuschi, N. Ludwig, A. Russo, P. Teruzzi, Statistical 212
 based procedure for defect sizing and experimental evalu-
 213 ation of the convective effects using Video Pulse Thermog-
 214 raphy. in: Proc. of 4th QIRT, Eurotherm Seminar no. 60,
 215 Lodz Poland, 1998. 216
 [6] F. Cernuschi, Ludwig, N. Russo, A. Teruzzi P, A critical 217
 analysis and possible modifications of two analytical models
 218 for defect sizing using Video Pulse Thermography. in: Proc.
 219 of 4th QIRT, Eurotherm Seminar no. 60, Lodz Poland,
 220 1998. 221
 [7] F.P. Incropera, D.P. DeWitt, Fundamentals of heat trans- 222
 223 fer, John Wiley and Sons, New York.

UNCORRECTED PROOF